Molecular Pharmacology Fast Forward. Published on October 1, 2004 as doi:10.1124/mol.104.004168

Dynamics of Ca^{2+}-dependent Cl^- Channel Modulation by Niflumic Acid in Rabbit Coronary Arterial Myocytes

Jonathan Ledoux, Iain A. Greenwood and Normand Leblanc

Department of Physiology, University of Montréal (J.L.) and Research Centre, Montréal Heart Institute (J.L.), Montréal, Québec, Canada, Department of Basic Medical Sciences, Pharmacology & Clinical Pharmacology (I.A.G.), St. George's Hospital Medical School, London, UK, & Department of Pharmacology (N.L.), Centre of Biomedical Research Excellence (COBRE), University of Nevada School of Medicine Reno, Nevada, USA

Molecular Pharmacology Fast Forward. Published on October 1, 2004 as DOI: 10.1124/mol.104.004168
This article has not been copyedited and formatted. The final version may differ from this version.

Running Title: *Dynamics of Vascular $I_{Cl(Ca)}$ Modulation by Niflumic Acid*

b) Corresponding Author:

Normand Leblanc, Ph.D.
Department of Pharmacology / Mail Stop 318
Center of Biomedical Research Excellence (COBRE)
Savitt Medical Sciences Building, Room 50
University of Nevada School of Medicine
Reno, Nevada 89557-0270

Tel.: 775-784-1420
Fax: 775-784-1620

E-mail: NLeblanc@med.unr.edu

c) Number of pages: 33 (including Title and Running Title pages)
Number of tables: 1
Number of figures: 9
Number of references: 31
Number of words in:
Abstract: 251
Introduction: 930
Discussion: 1875

d) List of Non-Standard Abbreviations:

A-9-C:	Anthracene-9-carboxylic acid
BK_{Ca}:	Large conductance calcium-activated potassium channel
$[Ca^{2+}]_i$:	Free intracellular calcium concentration
Cl_{Ca}:	Calcium-activated chloride channel
DCDPC:	Dichloro-diphenyl 2-carboxylic acid
DIDS:	4,4-diisothiocyanato-stilbene-2,2-disulphonic acid
EC_{50}:	Effective concentration of drug yielding 50% of maximal activation
E_{Cl}:	Equilibrium potential for chloride ions
EGTA:	Ethylene glycol-bis(2-aminoethylether)-N,N,N',N'-tetraacetic acid
Hepes:	4-(2-Hydroxyethyl) piperazine-1-ethanesulfonic acid
IC_{50}:	Effective concentration of drug yielding 50% of maximal inhibition
$I_{Cl(Ca)}$:	Calcium-activated chloride current
$[Mg^{2+}]_i$:	Free intracellular magnesium concentration
PSS:	Physiological salt solution
SITS:	Disodium 4-acetamido-4'-isothiocyanato-stilben-2,2'-disulfonate
TEA:	Tetraethylammonium chloride

Molecular Pharmacology Fast Forward. Published on October 1, 2004 as DOI: 10.1124/mol.104.004168
This article has not been copyedited and formatted. The final version may differ from this version.

Abstract

Calcium-activated chloride channels (Cl_{Ca}) are crucial regulators of vascular tone by promoting a depolarizing influence on the resting membrane potential of vascular smooth muscle cells. Niflumic acid (NFA), a potent blocker of Cl_{Ca} in vascular myocytes, was shown recently to cause inhibition and paradoxical stimulation of sustained $I_{Cl(Ca)}$ in rabbit pulmonary artery myocytes. The aims of the present study were to investigate whether NFA produced a similar dual effect in coronary artery smooth muscle cells, and to determine the concentration-dependence and dynamics of such a phenomenon. Sustained $I_{Cl(Ca)}$ evoked by intracellular Ca^{2+} clamped at 500 nM were dose-dependently inhibited by NFA (IC_{50} = 159 μM), and transiently augmented in a concentration-independent manner (10 μM to 1 mM) ~ 2-fold after NFA removal. However, the time to peak and duration of NFA-enhanced $I_{Cl(Ca)}$ increased in a concentration-dependent fashion. Moreover, the rate of recovery was reduced by membrane depolarization, suggesting the involvement of a voltage-dependent step in the interaction of NFA leading to stimulation of $I_{Cl(Ca)}$. Computer simulations based on a kinetic model involving low (K_i = 1.25 mM) and high (K_i < 30 μM) affinity sites could fairly well reproduce the properties of the NFA-modulated $I_{Cl(Ca)}$.

Molecular Pharmacology Fast Forward. Published on October 1, 2004 as DOI: 10.1124/mol.104.004168
This article has not been copyedited and formatted. The final version may differ from this version.

Introduction

Calcium-dependant chloride currents ($I_{Cl(Ca)}$) are expressed in various cell types including some types of vascular smooth muscle cells and are considered as a key player in the regulation of cell membrane potential. These currents are evoked by an elevation of intracellular Ca^{2+} concentration ($[Ca^{2+}]_i$) and have distinctive biophysical properties that include a discriminating selectivity pore that conforms to type I Eisenman sequence, voltage-dependent kinetics of activation and deactivation (Greenwood *et al*., 2001;Ledoux *et al*., 2003), a calcium sensitivity within the submicromolar range (EC_{50} ≈ 365 nM with full activation ≈ 600 nM $[Ca^{2+}]_i$) (Pacaud *et al*., 1992;Ledoux *et al*., 2003) and a small single channel conductance (1-3 pS) with multiple sub-conductance states (Klöckner, 1993;van Renterghem and Lazdunski, 1993;Hirakawa *et al*., 1999;Piper and Large, 2003). However the molecular identity of the channel underlying $I_{Cl(Ca)}$ in smooth muscle is still a matter of debate (see Britton *et al*., 2002). Consequently investigation of the physiological relevance of $I_{Cl(Ca)}$ relies upon the effectiveness of pharmacological tools. A number of chemically disparate compounds block $I_{Cl(Ca)}$ in smooth muscle cells ranging from stilbene derivatives (DIDS, SITS)(Hogg *et al*., 1994b), anthracene-9-carboxylic acid (A-9-C) (Hogg *et al*., 1994b) and fenamates (flufenamic acid, niflumic acid) (Hogg *et al*., 1994a;Greenwood and Large, 1995). Niflumic acid (NFA) is a non-steroidal anti-inflammatory drug that is recognized as the most potent inhibitor of $I_{Cl(Ca)}$ in smooth muscle cells owing to an IC_{50} within the low micromolar range (Hogg *et al*., 1994a; Greenwood and Large, 1995). Therefore, NFA has been widely used to assess the physiological role of these currents in the regulation of vascular tone (Criddle *et al*., 1996;Criddle *et al*., 1997;Yuan, 1997;Lamb and Barna, 1998;Remillard *et al*., 2000;Dai and Zhang, 2001).

Molecular Pharmacology Fast Forward. Published on October 1, 2004 as DOI: 10.1124/mol.104.004168
This article has not been copyedited and formatted. The final version may differ from this version.

However, NFA is not an ideal probe for investigating the role of $I_{Cl(Ca)}$, as this agent along with other members of the fenamate family, modulate a number of other ion channels. Niflumic acid and other fenamates stimulate large conductance Ca^{2+}-dependent K^+ channels (Ottolia & Toro, 1994; Hogg *et al.*, 1994a; Greenwood & Large, 1995). Flufenamic acid and tolfenamic acids relaxed guinea-pig tracheal contractions through a direct inhibition of voltage-gated Ca^{2+} channels (Li *et al.*, 1998). Niflumic acid stimulated Ca^{2+} release from internal stores in rat pulmonary artery smooth muscle cells (Cruikshank *et al.*, 2003), and was shown, along with NPPB and DIDS, to inhibit endothelin-1-induced contractions of rat pulmonary arterial myocytes by a mechanism independent of block of Cl_{Ca} channels (Kato *et al.*, 1999). Moreover, the IC_{50} for NFA block of spontaneously occurring $I_{Cl(Ca)}$ is significantly lower than that required to block $I_{Cl(Ca)}$ evoked by caffeine or an agonist such as norepinephrine (Large and Wang, 1996). This phenomenon is extended further when the channel is stimulated by a sustained level of [Ca^{2+}] provided by the pipette solution where a number of paradoxical effects are observed. In rabbit pulmonary myocytes NFA only blocked sustained $I_{Cl(Ca)}$ at positive potentials and augmented the tonic current at the holding potential of –50 mV (Piper *et al*., 2002). Upon washout of NFA there was a marked enhancement of current amplitude above control values that was associated with a marked increase in the activation kinetics. Similar effects were observed for the chemically related agent DCDPC (Piper *et al.*, 2002) whereas A-9-C, which inhibits $I_{Cl(Ca)}$ in a strongly voltage-dependent manner, produced a marked 3-fold increase in the deactivating tail current at –80 mV (Piper and Greenwood, 2003). These data suggest that in pulmonary artery myocytes, fenamates– and A-9-C–induced inhibition of $I_{Cl(Ca)}$ masks a parallel stimulation that is revealed either by washout of the drug (NFA) or by voltage-dependent dissociation from the channel (A-9-C). It is presently unknown whether the NFA–induced stimulation of $I_{Cl(Ca)}$ in pulmonary

artery myocytes (Piper *et al.*, 2002) is unique to that vascular smooth muscle preparation. Also, Piper *et al.* (2002) have used a slow superfusion system to monitor the effects of NFA on $I_{Cl(Ca)}$ and thus the true time course of stimulation of this current following washout of NFA is unclear. Finally, information on the concentration-dependence of the enhancing effect of NFA on $I_{Cl(Ca)}$ is lacking as Piper *et al.* (2002) have only examined the effect of a single concentration of NFA (100 μM).

The aim of the present study was to determine whether a similar anomalous effect of NFA was observed on sustained $I_{Cl(Ca)}$ by in rabbit coronary artery myocytes and to investigate the dynamics and concentration-dependence of this stimulation using a computer-assisted fast-flow superfusion system. We report here that the relative increase of $I_{Cl(Ca)}$ is independent of drug concentration whilst the time to reach the maximal stimulation and the duration of the enhanced state increased in a concentration-dependent manner. The rate of recovery from stimulation was also voltage-dependent with negative potentials accelerating recuperation from enhanced $I_{Cl(Ca)}$. We propose a model whereby NFA stimulates $I_{Cl(Ca)}$ by binding to high and low affinity sites which are occluded by the interaction of NFA with the inhibitory site. Preliminary results have been presented previously (Ledoux and Leblanc, 2002).

Molecular Pharmacology Fast Forward. Published on October 1, 2004 as DOI: 10.1124/mol.104.004168
This article has not been copyedited and formatted. The final version may differ from this version.

Methods and Materials

Isolation of coronary myocytes. Cells were freshly dissociated from coronary arteries isolated from New Zealand white rabbits (2-3 kg) that had been killed by anaesthetic overdose in accordance with Canadian and US regulations. All animal handling protocols received the approval of local ethics committees. Arterial myocytes were isolated from the left descending and circumflex coronary arteries. After dissection and removal of connective tissue the coronary arteries were cut into small strips and placed in a physiological salt solution (PSS) containing no added Ca^{2+} and 100 μM EGTA at 22^{o}C for 30 min. The coronary arteries were then incubated in a PSS containing 10 μM Ca^{2+} (no EGTA) and 1 mg ml^{-1} collagenase type 2 (Worthington, Lakewood, NJ) and 0.05 mg ml^{-1} protease type I (Sigma Chemical Co., St. Louis, MO) for 20-25 min at 35^{o}C. In all cases, cells were released by gentle agitation with a wide bore Pasteur pipette. Cells were stored at 4^{o}C and used within 6 h.

Electrophysiology. All experiments were carried out at room temperature (22-25°C) and all currents were recorded in the standard whole-cell variant of the voltage clamp technique using pClamp software (version 8.2, Axon Instruments Inc., Foster City, CA) and Axopatch-1D (Axon Instruments Inc.). Analysis was performed using the applicable software as well as Origin (version 5.0, Microcal, Northampton, MA). Current tracings and graph plots were all exported to CorelDraw (version 12, Corel Corp., Ottawa, Ontario) for processing of the figures. Solutions were delivered by gravity through a manifold perfusion system (Cell Micro Controls, Norfolk, VA) controlled by a homemade electronic switch box (Department of Biomedical Engineering, Montreal Heart Institute, Montreal, Quebec, Canada) that allowed to quickly modify the external medium surrounding the patched myocytes (complete exchange time of < 300 ms based on measurements of changes in junction potential of a patch pipette when switching from a NaCl-

based solution to a KCl-containing solution). Rapid replacement of external solutions was triggered and monitored using a Pentium II PC computer interfaced with a Digidata1200B acquisition system (Axon Instruments Inc.) and pClamp v8.2 software (Clampex).

Solutions. All experiments were carried out in K^+-free media. The external solution contained (mM): NaCl (130), $NaHCO_3$ (10), TEA-Cl (5.4), $MgCl_2$, (0.5), glucose (5.5), Hepes-NaOH (10; pH 7.35), $CaCl_2$, (1.8) and nifedipine (0.001). The pipette solution contained (mM): Cs-Aspartate (100), CsCl (20), TEA-Cl (20), Hepes-CsOH (5; pH 7.2), EGTA (10), Mg.ATP (5) and GTP.diNa (0.2). Free $[Ca^{2+}]_i$ was adjusted to 500 nM by adding $CaCl_2$ (7.7 mM) and $MgCl_2$ (0.77 mM), with free $[Mg^{2+}]_i$ set to 1 mM, as determined by the software WinMaxC (v.2.1, http://www.stanford.edu/~cpatton). As previously reported (Ledoux *et al*., 2003), buffered Ca^{2+} concentration in the pipette solution was independently verified using a Ca^{2+}-sensitive electrode (Thermo Orion, Model 93-20, Beverly, MA) and calibrated Ca^{2+} solutions available from a commercial source (World Precision Instruments, Inc., CALBUF-2, Sarasota, FL). Niflumic acid (NFA) and all enzymes were purchased from Sigma Chemical Company (St. Louis, MO). NFA was dissolved in dimethyl sulfoxide (DMSO; NFA stock solution = 100 mM) and the final DMSO concentration never exceeded 1%, a solvent concentration that did not alter the current in our conditions.

Computer simulations. The interaction of NFA with Cl_{Ca} channels was mathematically simulated using Markov chain kinetic models which were resolved numerically by Axon Engineer software (v. 2.11c, Aeon Software Inc., Madison, WI) run on Micron TransPort GX^+ laptop computer (Pentium III, 700 MHz). Simulations lasting up to 30 s were initiated from a holding potential of –50 mV under non-steady state conditions. Ordinary differential equations were simultaneously solved by the Gear numerical integration method using incremental time

Molecular Pharmacology Fast Forward. Published on October 1, 2004 as DOI: 10.1124/mol.104.004168
This article has not been copyedited and formatted. The final version may differ from this version.

steps of 10 μs. The specific parameters and equations used in the simulations are listed in Table 1.

Statistical analysis. All data are the mean ± s.e.m of *n* cells from greater than 2 animals. *Statistica* for Windows 99 (version 5.5, Tulsa, OK) was used to determine statistical significance between groups with one-way ANOVA test followed by a Fisher LSD *post-hoc* multiple range tests for repeated measures in multiple group comparisons. $p < 0.05$ was considered to be statistically significant.

Molecular Pharmacology Fast Forward. Published on October 1, 2004 as DOI: 10.1124/mol.104.004168
This article has not been copyedited and formatted. The final version may differ from this version.

Results

Under K^+-free internal and external conditions coronary myocytes dialyzed with an internal solution containing 500 nM free [Ca^{2+}] generated a sustained current at the holding potential of –50 mV that exhibited distinctive time-dependent outward relaxations upon depolarization followed by an exponentially declining inward current upon repolarization to –80 mV. This current is $I_{Cl(Ca)}$ evoked persistently by the pipette [Ca^{2+}] (500 nM) and has been characterized extensively in previous studies (Greenwood *et al*., 2001;Ledoux *et al*., 2003). Figure 1A shows that the application of 100 μM niflumic acid (NFA) with a fast-flow superfusion system quickly blocked both time-dependent outward current and tail components of $I_{Cl(Ca)}$ (see inset). Inhibition of $I_{Cl(Ca)}$ was observed with all concentrations of niflumic acid with an IC_{50} of 159 ± 48 μM (Fig. 1B). Upon washout of NFA, the current amplitude increased transiently beyond control values with a mean increase of 50 ± 8%, 73 ± 15% and 44 ± 9% for the instantaneous, late and tail current, respectively (n=11). This transient augmentation of current amplitude following a brief pulse of NFA was highly reproducible and could be repeated for the duration of the experiment (Fig. 1A). NFA washout not only modified $I_{Cl(Ca)}$ amplitude but also altered channel opening and closing rates (Figure 1C-*a*). Indeed, washout of NFA accelerated the activation kinetics at +90 mV and altered the kinetics of deactivation at –80 mV (Fig. 1C-*b* and *c*). In control conditions, the inward current relaxed following a monotonic time course with a time constant (τ) of 38 ± 2 ms, but decayed bi-exponentially following washout of NFA (Fig. 1C-*b* and *c*; mean τ values were 193 ± 25 ms and 21 ± 2 ms, n=10). These data show that the anomalous effects of NFA on sustained $I_{Cl(Ca)}$ described previously in pulmonary artery myocytes (Piper *et al*., 2002) are also apparent in coronary artery cells.

Molecular Pharmacology Fast Forward. Published on October 1, 2004 as DOI: 10.1124/mol.104.004168
This article has not been copyedited and formatted. The final version may differ from this version.

Concentration-dependence of NFA-induced $I_{Cl(Ca)}$ stimulation. The concentration- and time-dependence of the NFA stimulatory effect were performed on cells maintained at a test potential of +60 mV for 20 s and exposed to different concentrations of NFA (1 μM, 10 μM, 100 μM and 1 mM) for durations varying between 2 s and 10 s. Enhancement of $I_{Cl(Ca)}$ was only observed after washout of higher NFA concentrations greater than 1 μM (Fig. 2B-D). Moreover, the kinetics of the enhanced current was strongly dependent on the concentration of NFA applied. Thus the enhanced $I_{Cl(Ca)}$ generated upon washout of 10 μM NFA decayed monophasically after reaching its peak (Fig. 2B), whereas the relaxation of the stimulated current after removal of 100 μM NFA displayed a sustained phase superimposed on an initial rapid component (Fig. 2C). After washout of 1 mM NFA, the onset of stimulation was characterized by a markedly reduced rapid component followed by a slowly developing sustained phase of stimulation (Fig. 2D).

The relative increase of $I_{Cl(Ca)}$ amplitude upon washout of NFA did not vary as a function of the concentration of NFA applied. Thus, after 2 s applications in the same cell of 10 μM, 100 μM and 1 mM NFA, $I_{Cl(Ca)}$ increased respectively 1.9 ± 0.3, 2.1 ± 0.3 and 2.0 ± 0.2 fold. In contrast, the delay between the washout of drug and the maximal enhanced-$I_{Cl(Ca)}$ increased in a concentration-dependent manner (highlighted in the inset of Fig 3B). The time to reach the peak current increased significantly from 0.27 ± 0.03 s following washout of 10 μM NFA to 0.6 ± 0.2 s and 7 ± 1 s following washout of 100 μM and 1 mM NFA, respectively (n=7). Moreover the duration of the transient stimulated current upon washout of NFA was also concentration-dependent (Figs. 2 and 3C). The time for the stimulated current to decay by 50% of the maximal amplitude increased from 0.45 ± 0.03 s following washout of 10 μM NFA to 0.74 ± 0.08 s and 14 ± 1 s after removal of 100 μM and 1 mM NFA, respectively. From Figures 2 and 3 it is

Molecular Pharmacology Fast Forward. Published on October 1, 2004 as DOI: 10.1124/mol.104.004168
This article has not been copyedited and formatted. The final version may differ from this version.

obvious that for each NFA concentration the washout enhancement was not affected by changes in the duration of NFA application. These results highlight the complex dynamics associated with the stimulation of $I_{Cl(Ca)}$–produced by the washout of NFA.

Voltage-dependence of NFA-enhanced $I_{Cl(Ca)}$. We next sought to determine the voltage-dependence of the stimulation of $I_{Cl(Ca)}$ by NFA. In this series of experiments, cells were exposed to 100 μM NFA while being held at different membrane potentials, i.e. –60, +20, +60 and +90 mV from a holding potential of –50 mV (Fig. 4A–C and Fig. 5). These experiments revealed that the peak increase in $I_{Cl(Ca)}$ induced by a 10 s exposure to NFA was similar at all voltages examined (Fig. 5A). Shorter applications (2–8 s) of NFA revealed a similar pattern (data not shown). There was a trend, although not significant, that the time to peak stimulated current upon washout of NFA increased with membrane depolarization (Fig 5B). However, the time course of the stimulated current was clearly prolonged at positive relative to negative potentials as evident from analysis of the area under the curve of the stimulated current (Fig. 5C). Moreover, at +90 mV there was no significant decay of the stimulated current for the duration of this experiment (Fig. 4A).

Identity of NFA-enhanced current. It could be postulated that the current elicited upon washout of NFA was due to the *de novo* recruitment of a previously silent channel as opposed to modulation of an existent one. Therefore experiments were undertaken to determine if the stimulated current was equally sensitive to NFA as the control $I_{Cl(Ca)}$. Figure 6A shows a representative experiment where a cell was stepped to +60 mV and then NFA applied for 2 s. It can be clearly seen that the stimulated current evoked upon washout is rapidly inhibited by a repeat application of NFA to an extent observed for the control current. Similar results were observed in 3 other cells. Further experiments were undertaken to determine the reversal

Molecular Pharmacology Fast Forward. Published on October 1, 2004 as DOI: 10.1124/mol.104.004168
This article has not been copyedited and formatted. The final version may differ from this version.

potential of the current evoked upon washout of NFA. 500 ms after the application of NFA for 2 s, a ramp change in voltage (–50 mV to +50 mV, 250 ms) was imposed. The reversal potential of the enhanced $I_{Cl(Ca)}$ recorded from cells previously bathed in 100 μM (–15.8 ± 1.7 mV, n=6) or 1 mM NFA (–18.5 ± 1.6 mV, n=4) does not significantly differ from each other and are close to the theoretical value for the Cl^- equilibrium potential under our conditions (Greenwood *et al*., 2001;Ledoux *et al*., 2003). These data support the hypothesis that NFA is modulating an existing Cl channel.

Mathematical modeling of NFA interactions with I_{ClCa}. The experimental effects of NFA were simulated mathematically using a computer modeling method similar to that reported previously by our group (Remillard and Leblanc, 1996). Figure 7 displays the various kinetic schemes that were tested. Since the myocytes were dialyzed with a fixed intracellular Ca^{2+} concentration set at 500 nM, we simplified our theoretical analysis by focusing on the possible steps by which NFA interacts with the channels although we recognize that a more elaborate model of the channel (Arreola *et al.*, 1996;Kuruma and Hartzell, 2000) will have to be evaluated in the future. For all schemes tested, opening of the Ca^{2+}-activated Cl^- channel was modeled by single voltage-dependent reversible transition from closed (C) to open (O_1). Although a simple binding site model assuming a single binding site leading to block and stimulation (Fig. 7A) could fairly well reproduce the block and transient stimulation of $I_{Cl(Ca)}$ at 10 μM NFA, it could not account for the biphasic stimulation of $I_{Cl(Ca)}$ with 100 μM and 1 mM NFA. Alternative schemes were tested which assumed the existence of one inhibitory state and one (Fig. 7B and C), or two (Fig. 7D, E and F) stimulatory binding sites. For all the schemes shown in Fig. 7B through F, application of NFA first interacts with a binding site leading to current inhibition (B_1). State B_1 occludes the stimulation unless the drug is washed out quickly. We tested several

Molecular Pharmacology Fast Forward. Published on October 1, 2004 as DOI: 10.1124/mol.104.004168
This article has not been copyedited and formatted. The final version may differ from this version.

scheme variants which included a common high affinity blocking and stimulatory state, and a low affinity stimulatory state (Fig. 7C), and different schemes with a single inhibitory site, and two stimulatory binding sites with different affinities for NFA (Fig. 7D, E and F). Although these kinetic schemes were able to account for some aspects of the stimulation mediated by NFA, none of these could fairly well reproduce the concentration- and time-dependence of the block and enhancement of the current by this substance.

Figure 7G shows the model which best reproduced our experimental data. The equations describing the rate constants and other parameters used in the simulations are listed in Table 1. α_n and β_n are the rate constants for the kinetic transitions shown. The gating variables of the stimulated states O_2 and O_3, which are modeled as equivalent states, were set to 1. The fully activated non-stimulated open state O_1 was arbitrarily fixed at 0.7 although efforts to modify even slightly the gating values of the stimulated and non-stimulated states led to failure to model the interaction of NFA with the anion channel. Activation and deactivation were modeled by voltage-dependent transitions described by Boltzmann relationships. The model assumes the existence of high (ranging from 10 to 23 μM) and low (1.25 mM) affinity binding sites as indicated in Figure 7G. Binding of NFA was modeled using the Hill equation with a Hill coefficient of 1 ($O_1 \rightarrow B_2$, $O_2 \rightarrow B_1$) or 2 ($O_1 \rightarrow B_1$). The rate of unbinding of NFA from all bound states and the rates of recovery from stimulated to non-stimulated states were all assumed to be independent of NFA concentration.

Figure 8A and B show simulated current traces derived from the model with the four concentrations of NFA tested in our experiments elicited in response to 2 s (Fig. 8A) or 6 s (Fig. 8B) exposures to the drug as indicated below the normalized current traces. The voltage clamp protocol shown at the bottom was identical to that used in the experiments described in Figure 2.

Molecular Pharmacology Fast Forward. Published on October 1, 2004 as DOI: 10.1124/mol.104.004168
This article has not been copyedited and formatted. The final version may differ from this version.

The simulations were all initiated under non steady-state conditions which is why the gating variable for the closed state was set to 0.6. This allowed the simulation to begin with already active channels at the holding potential (–50 mV) in myocytes dialyzed with 500 nM Ca^{2+} or higher as previously shown by our group (Greenwood *et al.*, 2001; Ledoux *et al.*, 2003). Consistent with this scheme, step depolarization to +60 mV evoked an instantaneous current followed by a time-dependent $I_{Cl(Ca)}$ component (Greenwood *et al*., 2001;Ledoux *et al*., 2003)(this study, Figs. 1, 2, 4 and 6) that was well fitted by a single exponential with a time constant of 220 ms, a value similar to that previously published (Greenwood *et al.*, 2001;Ledoux *et al*., 2003). Application of NFA caused a rapid concentration-dependent block of the current which was more potent than actual data. Maximum block estimated by curve fitting to a Logistic function for experimental data and the model was respectively 62 ± 5 % and 96 ± 5 %. The model yielded a K_i that is approximately 5-fold lower (31 μM) than that calculated from actual data (159 μM). All attempts to adjust the parameters of the model listed in Table 1 to match the blocking ability of NFA to our measurements had deleterious consequences on the time- and dose-dependence of the NFA-induced stimulation of the current which was the main focus of our analysis.

Whereas washout of 1 μM NFA elicits little effect on the modeled current, washout of this drug when applied at concentrations in the range of 10 μM to 1 mM leads to a transient stimulation that reproduces our data reasonably well. Stimulated currents after washout of 10 or 100 μM NFA were much more transient than those evoked after exposure to 1 mM. Notice that a longer exposure to 100 μM NFA clearly led to a biphasic relaxation of the current (Fig. 8B, 3rd trace from top) as observed in experiments (Fig. 2C). The biphasic nature of the stimulated current after washout of 1 mM NFA, characterized by a rapid phase followed by a very slow

Molecular Pharmacology Fast Forward. Published on October 1, 2004 as DOI: 10.1124/mol.104.004168
This article has not been copyedited and formatted. The final version may differ from this version.

component (Fig. 2D), is also well accounted for by the model (Fig. 8B, 4th trace from top). Partial recovery of the current after the rapid onset of block was often observed during the application of NFA in the range of 10 μM to 1 mM (Fig. 2B, C and D). The model qualitatively reproduces this behavior with 100 μM and 1 mM NFA (Fig. 2B, 2nd and 3rd traces), which suggests that channels blocked by NFA (B_1 and B_2) may partially transit to the stimulated states (O_2 and O_3). Finally, the model is also able to simulate the impact of a double NFA exposure on the current (compare Fig. 8C with Fig. 6A) which again supports the concept that the control and stimulated currents are produced by the same underlying channels exhibiting distinct behaviors.

Figure 9 illustrates a quantitative comparison of the effects of NFA on recorded and simulated $I_{Cl(Ca)}$. Experimental and model data points are shown as filled and empty symbols. Except for a progressive increase of the simulated current as a function of exposure time to NFA with 1 mM (Fig. 9A-b) which diverged from the measured current which declined after NFA exposure times longer than 6 s, the model adequately describes the steep concentration-dependence of the stimulation between 1 μM and 1 mM; simulated data points generally fell within one standard deviation for each average measurement. Modeling this abrupt relationship could only be achieved by raising the Hill coefficient to 2 in the equation describing the rate constant α_2 (Fig. 7G; Table 1) of the high affinity binding site, which suggests that two or more NFA molecules may be necessary to induce stimulation. Figure 9B shows plots illustrating the time-dependent behavior of simulated versus measured $I_{Cl(Ca)}$. Measurements were carried out at washout times that elicited peak stimulated currents for each of the three NFA concentrations which were applied for 2 s. These graphs show reasonable agreement between the data and model with all three NFA concentrations, except for a discrepancy observed at the earliest washout time with 100 μM.

Molecular Pharmacology Fast Forward. Published on October 1, 2004 as DOI: 10.1124/mol.104.004168
This article has not been copyedited and formatted. The final version may differ from this version.

Discussion

Niflumic acid exerts a dual influence on Cl_{Ca} channels in coronary myocytes. A number of chemically diverse agents block Ca^{2+}-activated Cl^- channels and NFA is unequivocally considered to be the most potent blocker of this conductance in vascular smooth muscle cells (Large and Wang, 1996). The data reported herein show that in coronary artery myocytes a sustained Ca^{2+}-activated Cl^- current characterized extensively in previous reports is modulated in a paradoxical manner by the chloride channel blocker niflumic acid. Analysis of the dose-dependent block of $I_{Cl(Ca)}$ revealed an IC_{50} that was higher (159 μM) than that determined for the inhibitory action of NFA on spontaneous transient inward currents or STICs (~ 2–5 μM; Hogg *et al*., 1994a;Greenwood and Large, 1995), which results from the transient activation of Cl_{Ca} channels by Ca^{2+} sparks (Gordienko *et al.*, 1999). This diminished potency of NFA to inhibit $I_{Cl(Ca)}$ was also noticed by Piper *et al.* (Piper *et al*., 2002) in rabbit pulmonary myocytes dialyzed with elevated $[Ca^{2+}]_i$ (250 nM – 1 μM). Whether the higher efficacy of NFA for blocking STICs relative to $I_{Cl(Ca)}$ elicited by a sustained elevated intracellular Ca^{2+} level is due to the much higher Ca^{2+} concentrations (tens of micromolar) generated by Ca^{2+} sparks (Jaggar *et al.*, 2000) or the ability of NFA to interfere with Ca^{2+} release from internal stores (Cruickshank *et al.*, 2003) remains to be investigated. An alternative possibility is that under conditions of a sustained rise in $[Ca^{2+}]_i$, NFA may stimulate the Cl^- channels, an effect that would be partially obstructed by the inhibition. The study by Piper *et al.* (Piper *et al.*, 2002) demonstrated that washout of NFA enhances $I_{Cl(Ca)}$ in pulmonary myocytes and postulated that the higher open probability of Cl_{Ca} channels elicited by a sustained rise in $[Ca^{2+}]_i$ may tilt the balance towards the stimulatory effect. Our data support this hypothesis as the rapid block exerted by NFA was often followed by a

Molecular Pharmacology Fast Forward. Published on October 1, 2004 as DOI: 10.1124/mol.104.004168
This article has not been copyedited and formatted. The final version may differ from this version.

partial recovery of the current, which suggests that the net current recorded with NFA was the product of a superimposed inhibition and stimulation by the drug.

NFA at concentrations between 10 μM to 1 mM produced an ≈ 2-fold increase in $I_{Cl(Ca)}$ elicited by 500 nM $[Ca^{2+}]_i$. Whilst the relative increase of $I_{Cl(Ca)}$ was independent of NFA concentration, the time to reach the peak current increased in a concentration-dependent manner. Furthermore, the time needed to recover from the enhanced state increased in a concentration-dependent manner. These data reflect an anomalous modulation of a Ca^{2+}-activated Cl^- channels by NFA as the NFA-increased current reversed near the predicted E_{Cl} confirming that the underlying channels were permeable to Cl^-. Moreover, the current enhanced by NFA was equally blocked by a second exposure to this compound. These findings corroborate the earlier observations of Piper *et al* (2002) showing that the current generated by the removal of NFA was not due to the *de novo* activation of another conductance.

Voltage-dependence of NFA-enhanced anion current. The relative magnitude of NFA-enhanced $I_{Cl(Ca)}$ was independent of membrane potential in the range of –60 to +90 mV. However, the rate of current recovery following NFA washout was clearly voltage-dependent, with membrane depolarization delaying the return of the current to baseline. One possibility to explain these results is that the dissociation of NFA is voltage-dependent, with membrane depolarization reducing the rate of unbinding from its binding site(s). An interaction of this drug with the hydrophilic channel pore or extracellular vestibular portion has been postulated (Greenwood and Large, 1995;Hogg *et al*., 1994a). Piper *et al.* (Piper *et al*., 2002) showed that intracellular application of NFA (100 μM) was ineffective at modifying $I_{Cl(Ca)}$ in pulmonary myocytes supporting the idea that NFA modulates Cl_{Ca} channels by accessing one or several binding sites located primarily near the outer mouth of the channel pore. It is possible that NFA

Molecular Pharmacology Fast Forward. Published on October 1, 2004 as DOI: 10.1124/mol.104.004168
This article has not been copyedited and formatted. The final version may differ from this version.

may be interacting with a binding site(s) through an electrostatic interaction that is modulated by the transmembrane electric field, or by the state of Ca^{2+}- and voltage-dependent gating of the channels.

Mechanism of action of niflumic acid on Cl_{Ca} channels. Until the molecular nature of native Ca^{2+}-activated Cl^- channels is resolved, we can only speculate on the possible mechanism by which NFA mediates its effects on the channels. It is possible that the stimulation by NFA is caused by a leftward shift of the voltage-dependence of $I_{Cl(Ca)}$ leading to saturation at higher $[Ca^{2+}]_i$, although we cannot rule out the recruitment of silent channels, and/or an increase in single-channel conductance. In agreement with this idea, Piper *et al.* (Piper *et al*., 2002) showed that the stimulatory effects of NFA were abolished by increasing $[Ca^{2+}]_i$ from 500 nM to 1 μM in pulmonary myocytes which would increase the voltage-dependent availability of $I_{Cl(Ca)}$. Alternatively, NFA could exert a dual effect by inhibiting both Cl_{Ca} channels and the ryanodine and/or IP_3 Ca^{2+} release channels. In the presence of NFA, Cl_{Ca} channels would be blocked and the SR Ca^{2+} load would increase due to reduced Ca^{2+} leakage. Stimulation of $I_{Cl(Ca)}$ after washout of NFA would then result from a transient subsarcolemmal Ca^{2+} release event produced by relief of block of the Ca^{2+} release channels, even though bulk free $[Ca^{2+}]_i$ is highly buffered by BAPTA. Arguments against this hypothesis are: 1) our inability to ever detect STICs in our experiments, 2) the time course of stimulation of $I_{Cl(Ca)}$ by NFA was highly voltage-dependent (Fig. 5), and 3) NFA was recently shown to enhance rather than inhibit Ca^{2+} release in rat pulmonary myocytes (Cruickshank *et al.*, 2003).

Although the hypothesis of a single binding site is possible, we rather favor the hypothesis that NFA is interacting with more than one binding site, each with different affinities. We carried out mathematical simulations that might account for our observations. Only the working model

Molecular Pharmacology Fast Forward. Published on October 1, 2004 as DOI: 10.1124/mol.104.004168
This article has not been copyedited and formatted. The final version may differ from this version.

shown in Figure 7G could well describe most of the properties of NFA-modulated $I_{Cl(Ca)}$ in our preparation. At low concentrations of NFA (≤ 10 μM), the molecules would only bind to the high affinity site, which would cause a conformational change in the protein leading to enhanced activity but this effect would be mostly masked by channel occlusion. A small but significant number of channels would enter the stimulated state O_2 and thus lead to reduced blockade by the compound. When NFA is washed out, most channels would return to the normal control open state O_1 while others that have adopted a new conformational change favoring stimulation would transit to O_2; the slow and transient nature of $I_{Cl(Ca)}$ would arise from the slow unbinding of NFA ($B_1 \rightarrow O_2$) and slow rate constant describing the return of the stimulated state to the normal state ($O_2 \rightarrow O_1$). At 100 μM NFA, some NFA molecules are beginning to interact with a second lower affinity binding site that also leads to block (B_2) and stimulation (O_3). The very slow kinetics of unbinding of NFA ($B_2 \rightarrow O_3$) and recovery of the current from the stimulated state ($O_3 \rightarrow O_1$) could explain the appearance of a slower kinetically distinct phase of transient stimulation of $I_{Cl(Ca)}$ after washout of NFA. This becomes even more apparent after washout of 1 mM NFA. The onset of stimulation is now clearly biphasic with a rapid and a slow phase, both of which are well described by the model. The enhanced contribution of a slower phase with a correspondingly reduced rapid component is also consistent with the existence of two mutually exclusive binding sites.

Although useful as an initial working hypothesis to describe the complex interaction of NFA with native Cl_{Ca} channels, the model offers no clues on the molecular mechanisms that are involved in the NFA-induced alterations in channel activity. So far, two kinetic models have been postulated to describe the Ca^{2+}- and voltage-dependence of Ca^{2+}-activated Cl^- channels in parotid acinar cells (Arreola *et al*., 1996) and *Xenopus* oocytes (Callamaras and Parker, 2000;

Molecular Pharmacology Fast Forward. Published on October 1, 2004 as DOI: 10.1124/mol.104.004168
This article has not been copyedited and formatted. The final version may differ from this version.

Kuruma and Hartzell, 2000). These two models are divergent in that one assumes that activation of Cl_{Ca} channels by voltage-dependent binding of several Ca^{2+} ions (Arreola *et al.*, 1996; Callamaras and Parker, 2000) whereas the other postulates that Ca^{2+} binding is voltage-independent while unbinding involves a voltage-dependent step (Kuruma and Hartzell, 2000). Unfortunately such a detailed description of the behavior of Cl_{Ca} channels in vascular smooth muscle is still awaiting and is complicated by the very small unitary conductance of the channels (~ 1–3 pS)(Large and Wang, 1996;Klöckner, 1993;van Renterghem and Lazdunski, 1993;Hirakawa *et al*., 1999;Piper and Large, 2003) and the fact that they are regulated by phosphotransferase reactions involving calmodulin-dependent protein kinase II (CaMKII)(Greenwood *et al.*, 2001) and calcineurin (Ledoux *et al.*, 2003), both of which are activated by intracellular Ca^{2+}. Although additional experiments are required to answer this question, a likely explanation for the effects of NFA may be that the antagonist promotes Ca^{2+} binding and/or reduces the unbinding of Ca^{2+}, one of which is voltage-dependent, leading to an increase in the open probability. Consistent with this hypothesis was the observation that activation and deactivation kinetics of $I_{Cl(Ca)}$ were respectively enhanced and reduced following washout of NFA and this is similar to the effects of an elevation of intracellular Ca^{2+} to near saturation levels on $I_{Cl(Ca)}$ in other cell types (Arreola *et al*., 1996;Kuruma and Hartzell, 2000).

Pharmacological relevance of our findings. Determination of the role of Cl_{Ca} channels in vascular smooth muscle has been hampered by the lack of truly specific pharmacological probes. Our data provide evidence that niflumic acid, the most potent inhibitor of these channels in vascular myocytes (Large and Wang, 1996), also induces a complex stimulation of the channels in rabbit coronary smooth muscle cells, an effect which is masked by its faster inhibitory action, but can be revealed upon rapid washout of the drug. Our work highlights the caveats about the

use of this tool to study the physiological role of Cl_{Ca} channels. In studies carried out to investigate their functional role, NFA was shown to alleviate agonist-induced tone which is caused by a sustained elevation in $[Ca^{2+}]_i$. Such a condition reduces the ability of NFA to block $I_{Cl(Ca)}$ as compared to its effect on STICs (Hogg *et al*., 1994a;Greenwood and Large, 1995). Our experimental and simulated data support the notion that the reduced efficacy of NFA as an inhibitor may be due to partial stimulation of the channels in the presence of the drug. Therefore, lack of effect of NFA in contraction studies with multicellular preparations should not be taken as evidence against a physiological role of Cl_{Ca} in determining vascular smooth muscle tone.

Acknowledgements

We are thankful to Dr Rémy Sauvé for his helpful comments and suggestions during the course of this work.

References

Arreola J, Melvin J E and Begenisich T (1996) Activation of calcium-dependent chloride channels in rat parotid acinar cells. *J Gen Physiol* **108**: 35-47.

Britton FC, Ohya S, Horowitz B and Greenwood I A (2002) Comparison of the properties of CLCA1 generated currents and $I_{Cl(Ca)}$ in murine portal vein smooth muscle cells. *J Physiol* **539**: 107-117.

Callamaras N and Parker I (2000) Ca^{2+}-dependent activation of Cl^- currents in *Xenopus* oocytes is modulated by voltage. *Am J Physiol Cell Physiol* **278**: C667-C675.

Criddle DN, deMoura R S, Greenwood I A and Large W A (1996) Effect of niflumic acid on noradrenaline-induced contractions of the rat aorta. *Br J Pharmacol* **118**: 1065-1071.

Criddle DN, deMoura R S, Greenwood I A and Large W A (1997) Inhibitory action of niflumic acid on noradrenaline- and 5-hydroxytryptamine-induced pressor responses in the isolated mesenteric vascular bed of the rat. *Br J Pharmacol* **120**: 813-818.

Cruickshank SF, Baxter L M and Drummond R M (2003) The Cl^- channel blocker niflumic acid releases Ca^{2+} from an intracellular store in rat pulmonary artery smooth muscle cells. *Br J Pharmacol* **140**: 1442-1450.

Dai Y and Zhang J H (2001) Role of Cl^- current in endothelin-1-induced contraction in rabbit basilar artery. *Am J Physiol Heart Circ Physiol* **281**: H2159-H2167.

Gordienko DV, Zholos A V and Bolton T B (1999) Membrane ion channels as physiological targets for local Ca^{2+} signalling. *J Microscopy Oxford* **196**: 305-316.

Greenwood I, Ledoux J and Leblanc N (2001) Differential regulation of Ca^{2+}-activated Cl^- currents in rabbit arterial and portal vein smooth muscle cells by Ca^{2+}-calmodulin-dependent kinase. *J Physiol* **534.2**: 395-408.

Greenwood IA and Large W A (1995) Comparison of the effects of fenamates on Ca-activated chloride and potassium currents in rabbit portal vein smooth muscle cells. *Br J Pharmacol* **116**: 2939-2948.

Hirakawa Y, Gericke M, Cohen R A and Bolotina V M (1999) Ca^{2+}-dependent Cl^- channels in mouse and rabbit aortic smooth muscle cells: regulation by intracellular Ca^{2+} and NO. *Am J Physiol Heart Circ Physiol* **277**: H1732-H1744.

Hogg RC, Wang Q and Large W A (1994a) Action of niflumic acid on evoked and spontaneous calcium-activated chloride and potassium currents in smooth muscle cells from rabbit portal vein. *Br J Pharmacol* **112**: 977-984.

Hogg RC, Wang Q and Large WA (1994b) Effects of Cl channel blockers on Ca-activated chloride and potassium currents in smooth muscle cells from rabbit portal vein. *Br J Pharmacol* **111**: 1333-1341.

Jaggar JH, Porter V A, Lederer W J and Nelson M T (2000) Calcium sparks in smooth muscle. *Am J Physiol Cell Physiol* **278**: C235-C256.

Kato K, Evans A M and Kozlowski R Z (1999) Relaxation of endothelin-1-induced pulmonary arterial constriction by niflumic acid and NPPB: Mechanism(s) independent of chloride channel block. *J Pharmacol Exp Ther* **288**: 1242-1250.

Klöckner U (1993) Intracellular calcium ions activate a low-conductance chloride channel in smooth-muscle cells isolated from human mesenteric artery. *Pflügers Arch Eur J Physiol* **424** : 231-237.

Kuruma A and Hartzell H C (2000) Bimodal control of a Ca^{2+}-activated Cl^- channel by different Ca^{2+} signals. *J Gen Physiol* **115**: 59-80.

Lamb FS and Barna T J (1998) Chloride ion currents contribute functionally to norepinephrine-induced vascular contraction. *Am J Physiol Heart Circ Physiol* **275**: H151-H160.

Large WA and Wang Q (1996) Characteristics and physiological role of the Ca^{2+}-activated Cl^- conductance in smooth muscle. *Am J Physiol Cell Physiol* **271**: C435-C454.

Ledoux J, Greenwood I, Villeneuve L R and Leblanc N (2003) Modulation of Ca^{2+}-dependent Cl^- channels by calcineurin in rabbit coronary arterial myocytes. *J Physiol* **552.3**: 701-714.

Ledoux J and Leblanc N (2002) Dual modulation of calcium-activated chloride channels by niflumic acid in rabbit coronary artery myocytes. *J Physiol* **543P**: S155.

Li L, Vapaatalo H, Vaali K, Paakkari I and Kankaanranta H (1998) Flufenamic and tolfenamic acids and lemakalim relax guinea-pig isolated trachea by different mechanisms. *Life Sci* **62**: PL303-PL308.

Ottolia M and Toro L (1994) Potentiation of large conductance K_{Ca} channels by niflumic, flufenamic, and mefenamic acids. *Biophys J* **67**: 2272-2279.

Pacaud P, Loirand G, Grégoire G, Mironneau C and Mironneau J (1992) Calcium-dependence of the calcium-activated chloride current in smooth muscle cells of rat portal vein. *Pflügers Arch*

Eur J Physiol **421**: 125-130.

Piper AS and Greenwood I A (2003) Anomalous effect of anthracene-9-carboxylic acid on calcium-activated chloride currents in rabbit pulmonary artery smooth muscle cells. *Br J Pharmacol* **138**: 31-38.

Piper AS, Greenwood I A and Large WA (2002) Dual effect of blocking agents on Ca^{2+}-activated Cl^- currents in rabbit pulmonary artery smooth muscle cells. *J Physiol* **539**: 119-131.

Piper AS and Large W A (2003) Multiple conductance states of single Ca^{2+}-activated Cl^- channels in rabbit pulmonary artery smooth muscle cells. *J Physiol* **547**: 181-196.

Remillard CV and Leblanc N (1996) Mechanism of inhibition of delayed rectifier K^+ current by 4-aminopyridine in rabbit coronary myocytes. *J Physiol* **491**: 383-400.

Remillard CV, Lupien M A, Crépeau V and Leblanc N (2000) Role of Ca^{2+}- and swelling-activated Cl^- channels in α_1-adrenoceptor-mediated tone in pressurized rabbitmesenteric arterioles. *Cardiovasc Res* **46**: 557-568.

van Renterghem C and Lazdunski M (1993) Endothelin and vasopressin activate low conductance chloride channels in aortic smooth muscle cells. *Pflügers Arch Eur J Physiol* **425**: 156-163.

Yuan XJ (1997) Role of calcium-activated chloride current in regulating pulmonary vasomotor tone. *Am J Physiol Lung Cell Mol Physiol* **272**: L959-L968.

Footnotes

This work was supported by a Doctoral Studentship Award (to JL) from the Canadian Institute of Health Research (CIHR), a Wellcome Trust Research Career Development Fellowship to IAG (# 53793), and grants to NL from the CIHR (MOP-10863), the Montréal Heart Institute Fund, the Western Affiliate of the American Heart Association (0355060Y), and the Center of Biomedical Research Excellence (COBRE; NCRR 5 P20 RR15581), University of Nevada School of Medicine, Reno, Nevada. Please send reprint requests to: Normand Leblanc, Department of Pharmacology/Mail Stop 318, Center of Biomedical Research Excellence (COBRE), Savitt Medical Sciences Building, University of Nevada School of Medicine, Reno, Nevada 89557-0270.

Molecular Pharmacology Fast Forward. Published on October 1, 2004 as DOI: 10.1124/mol.104.004168
This article has not been copyedited and formatted. The final version may differ from this version.

Legends for Figures

Figure 1. *Block and stimulation of Ca^{2+}-activated Cl^- current by niflumic acid in rabbit coronary myocytes dialyzed with 500 nM $[Ca^{2+}]_i$.*

A. Time course of peak outward current recorded at +90 mV every 10 s in coronary smooth muscle cells dialyzed with 500 nM $[Ca^{2+}]_i$. 100 μM NFA (NFA) was applied using a fast-flow superfusion system for the period denoted by the bar. *Inset:* Sample traces obtained in control (*a*), presence (*b*) and following washout of 100 μM NFA (*c*), respectively. **B.** Concentration-dependence of the inhibitory effects of NFA on $I_{Cl(Ca)}$ recorded at +60 mV. Data were obtained from experiments similar to those illustrated in Figure 2. The solid line passing through the points is a Logistic function fit to the data with the following parameters: $Y = 76.1 / [1 + (x / 159)^{0.42}]$. For NFA concentrations = 1 μM, 10 μM, 100 μM and 1 mM, n = 11, 7, 7 and 7, respectively. **C**. Effects of NFA removal on activation and deactivation kinetics of $I_{Cl(Ca)}$. *a*. Sample traces of $I_{Cl(Ca)}$ evoked by the protocol used in A in the absence (control) and following washout of 100 μM NFA. Panels *b* and *c* show bar graphs representing the means time constants of activation (+90 mV) and deactivation (–80 mV), respectively before (control) and after (washout) exposure to 100 μM NFA of experiments similar as shown in *a* (n=10).

Figure 2. *Dynamics of the stimulated current evoked upon washout of NFA.*

Sample traces of $I_{Cl(Ca)}$ evoked by a 22 s depolarizing step to +60 mV (HP = –50 mV) followed by a repolarizing step to –50 mV for 8 s every 60 s (A, B and C) or 90 s (D) as displayed at the bottom of the figure. After 2 s, 1, 10, 100 μM or 1 mM NFA (A, B, C and D, respectively) was applied for increasing durations (2 s increment) using a fast flow superfusion system. Vertical

Molecular Pharmacology Fast Forward. Published on October 1, 2004 as DOI: 10.1124/mol.104.004168
This article has not been copyedited and formatted. The final version may differ from this version.

calibrations express the ratio of current amplitude relative to the level reached immediately before the application of NFA.

Figure 3. *Concentration-dependence of enhanced $I_{Cl(Ca)}$ dynamics induced by NFA washout in coronary myocytes depolarized to +60 mV.*

A. Plot reporting the mean relative increase of $I_{Cl(Ca)}$ in coronary myocytes induced by washout of NFA (1 μM, 10 μM, 100 μM and 1 mM, n= 11, 7, 7 and 7, respectively) calculated as the peak current amplitude at +60 mV following removal of NFA normalized to the current value prior to the application of NFA (for 2 to 10 s) as described in Figure 2. ANOVA statistical analysis for repeated measure revealed a significant difference between the groups with a ** $p < 0.01$. **B**. Graph illustrating the time delay between the washout of drug and the peak amplitude of enhanced $I_{Cl(Ca)}$ after washout of NFA (10, 100 μM and 1 mM, n=7) applied for 2 to 10 s. *Inset*. Magnified view of sample traces of cells exposed to 10 μM, 100 μM and 1 mM NFA for 2 s to illustrate the concentration-dependent time to peak amplitude of enhanced $I_{Cl(Ca)}$. ANOVA statistical analysis for repeated measures revealed a significant difference between the groups with ** $p < 0.001$. **C**. Bar graph showing the mean decay kinetics of enhanced $I_{Cl(Ca)}$ in cells exposed to 10 μM, 100 μM and 1 mM NFA for 2 s. The time–dependent relaxation was calculated as the period required for peak enhanced $I_{Cl(Ca)}$ to decline by 50% . One-way ANOVA statistical analysis revealed a significant difference between the 3 groups with *** $p < 0.001$.

Figure 4. *Voltage-dependence of the enhanced $I_{Cl(Ca)}$ after washout of NFA.*

A. Sample traces of $I_{Cl(Ca)}$ evoked by a 22 s step to –60 mV (HP = –50 mV) followed by a repolarizing step to –50 mV for 8 s every 60 s as displayed under the traces. After 2 s, cells were

Molecular Pharmacology Fast Forward. Published on October 1, 2004 as DOI: 10.1124/mol.104.004168
This article has not been copyedited and formatted. The final version may differ from this version.

exposed to 100 μM NFA for 2 s up to 10 s with 2 s increments followed by the rapid removal of drug from the external medium using a fast flow superfusion system as depicted over the traces. **B** and **C**. Similar to A except that the cells were depolarized to +20 mV and +90 mV for 22 s (B and C, respectively) as illustrated under the traces.

Figure 5. *Quantitative analysis of the voltage-dependence of enhanced $I_{Cl(Ca)}$ induced by 100 μM NFA washout in coronary myocytes.*

A. Bar graph reporting the mean relative increase in $I_{Cl(Ca)}$ induced after washout of 100 μM NFA applied for 10 s in myocytes held at –60 (filled column), +20 (hollow column), +60 (cross-hatched column) and +90 mV (light grey column)(n=5, 5, 7 and 5 respectively) and calculated as the peak current amplitude following removal of NFA normalized to the current value just prior to exposure to drug as described in Figure 4. **B**. Bar graph summarizing the mean delay in milliseconds between the removal of drug and the peak amplitude of enhanced $I_{Cl(Ca)}$ after washout of 100 μM NFA applied for 10 s in myocytes held at –60 (filled column), +20 (hollow column), +60 (cross-hatched column) and +90 mV (light grey column)(n = 5, 5, 7 and 5 respectively). **C**. Bar graph reporting the mean integrated current stimulated by NFA washout measured at –60 (filled column), +20 (hollow column), +60 (cross-hatched column) and +90 mV (light grey column)(n = 5, 5, 7 and 5 respectively). One-way ANOVA statistical analyses revealed a significant difference between the 3 groups with *** $p < 0.001$.

Figure 6. *Properties of NFA-enhanced $I_{Cl(Ca)}$.*

A. Effect of a 2 s application of NFA on $I_{Cl(Ca)}$ recorded at +60 mV. 500 ms after washout of NFA, the augmented current was blocked by a repeat application of NFA to a similar degree as

the control current. **B**. Generation of a ramp change in voltage 4.5 s after washout of NFA allowed the reversal potential of the stimulated current to be determined. *Inset:* Relative current amplitude plotted as a function of the membrane potential imposed by the ramp protocol (reversal potential in this cell was –16 mV).

Figure 7. *The different kinetic schemes tested in computer simulations.*

C, O_n, B_n reflect closed, open and blocked kinetic states. NFA, niflumic acid. In panel G, α_n and β_n are respectively the forward and backward rate constants describing the individual state transitions. The equations describing all the rate constants shown on this scheme are listed in Table 1.

Figure 8. *Simulation of the effects of niflumic acid on Ca^{2+}-activated Cl^- currents using the model described in the text.*

A. Normalized simulated currents elicited by 22 s voltage clamp steps to +60 from holding potential of –50 mV (bottom trace). In these simulations, a 2 s exposure to either 1 μM (top trace), 10 μM (2^{nd} trace from top), 100 μM (3^{rd} trace from top) or 1 mM (4^{th} trace from top) niflumic acid (NFA) was implemented 2 s after membrane potential was stepped to +60 mV as illustrated by the trace immediately above the voltage clamp protocol. **B.** Identical to panel A except that each concentration of NFA was applied for 6 s. **C.** Simulation showing the effect of a double exposure to 100 μM NFA. The two exposures (middle trace) lasted 1 s and were interspersed by a 500 ms gap. The voltage clamp protocol shown at the bottom was identical to those described in panels A and B.

Molecular Pharmacology Fast Forward. Published on October 1, 2004 as DOI: 10.1124/mol.104.004168
This article has not been copyedited and formatted. The final version may differ from this version.

Figure 9. *Comparison of the effects of NFA on recorded and simulated $I_{Cl(Ca)}$.*

A. Graphs showing the time- and dose-dependence of the NFA-induced stimulation of recorded and simulated $I_{Cl(Ca)}$ after washout of the drug. Experimental data points are reproduced from Figure 3. A 22 s steps to +60 mV was applied from HP = –50 mV. Two seconds after the onset of the depolarizing step, NFA was applied for between 2 and 10 s at the concentrations indicated at the top of each graph. Notice the fairly good correlation between experimental (filled symbols) and simulated (open symbols) data. **B.** Graphs showing the time course of NFA-enhanced recorded (filled symbols) and simulated (empty symbols) $I_{Cl(Ca)}$ after washout of 10 μM (*a*), 100 μM (*b*) or 1 mM (*c*) NFA (2 s exposure). The selected washout times chosen correspond to the time to peak measurements based on the experiments described in Figure 3. Except for the earliest washout time point with 100 μM NFA where a significant deviation was noticed, the model generally well reproduced the experimental data.

Molecular Pharmacology Fast Forward. Published on October 1, 2004 as DOI: 10.1124/mol.104.004168
This article has not been copyedited and formatted. The final version may differ from this version.

Table 1. *Parameters used to compute the mathematical model describing the inhibition and stimulation of $I_{Cl(Ca)}$ by niflumic acid*

	Units
Permeability and selectivity	
$P_{Cl(Ca)}\ max = 0.01$	$\mu m\ ms^{-1}$
$E_{Cl} = -30$	mV
Values of gating variables	
$C = 0.6$	
$O_1 = 0.7$	
$B_1 = 0$	
$B_2 = 0$	
$O_2 = 1$	
$O_3 = 1$	
Activation and deactivation	
$\alpha_1\ (V) = 0.0075 / \{1 + \exp [-0.1 * (V - 50)]\}$	ms^{-1}
$\beta_1\ (V) = 0.1 / \{1 + \exp [0.1 * (V + 80)]\}$	ms^{-1}
High affinity binding of NFA and unbinding	
$\alpha_2\ ([NFA]) = [NFA]^2 / \{[NFA]^2 + 0.023^2\}$	ms^{-1}
$\beta_2 = 0.5$	ms^{-1}
$\alpha_3 = 0.058$	ms^{-1}
$\beta_3\ ([NFA]) = 0.05 * \{[NFA] / \{[NFA] + 0.01\}$	ms^{-1}
Low affinity binding of NFA and unbinding	
$\alpha_4\ ([NFA]) = 0.00325 * \{[NFA] / \{[NFA] + 1.25\}$	ms^{-1}
$\alpha_5 = 0.0004$	ms^{-1}
Recovery from high affinity and fast binding of NFA	
$\alpha_6 = 0.0006$	ms^{-1}
Recovery from low affinity and slow binding of NFA	
$\alpha_7 = 0.0001$	ms^{-1}

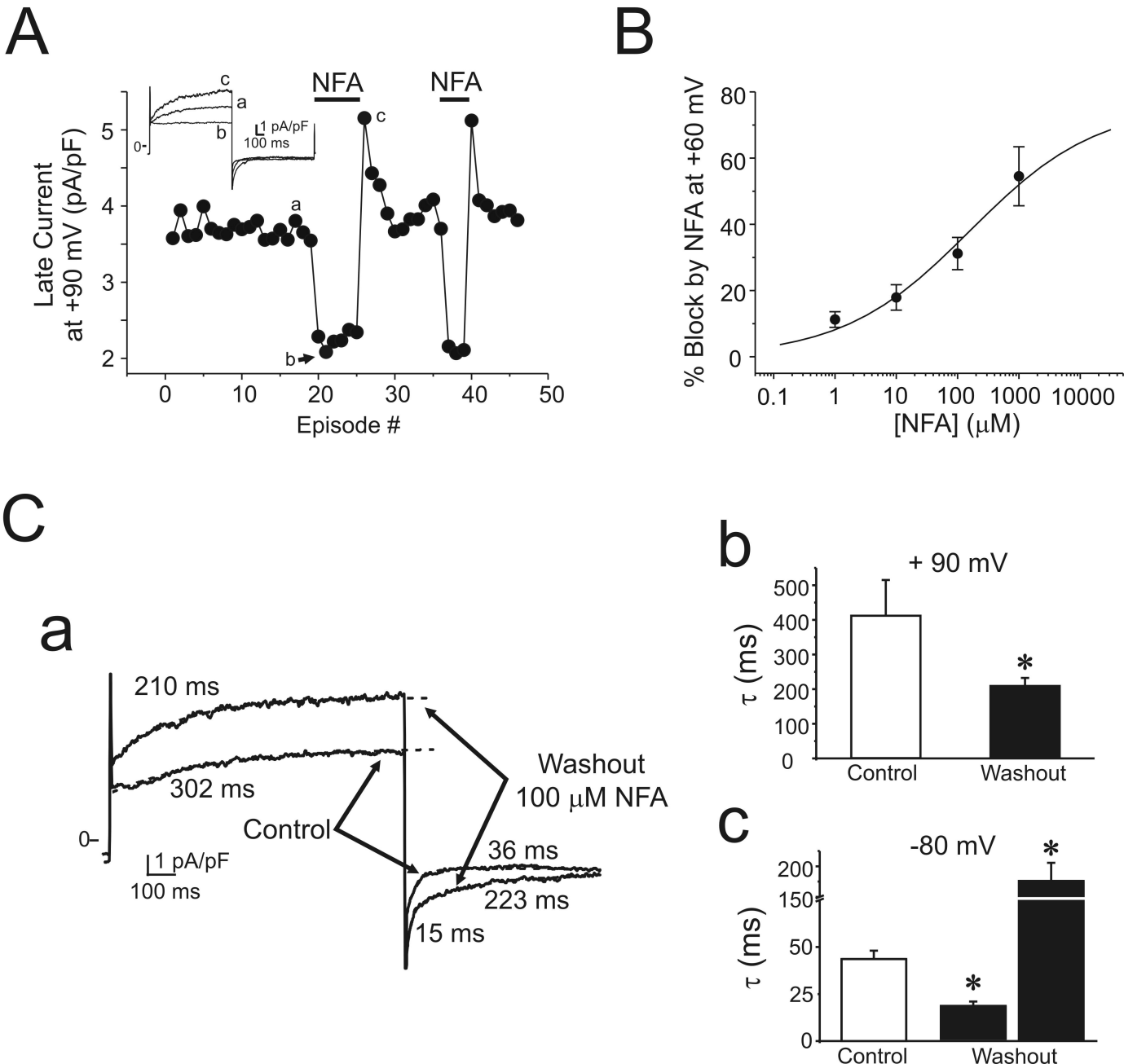
A
NFA
NFA
c
a
b
1 pA/pF
100 ms
0
Late Current
at +90 mV (pA/pF)
Episode #
B
% Block by NFA at +60 mV
[NFA] (μM)
C
a
210 ms
302 ms
Control
Washout
100 μM NFA
36 ms
223 ms
15 ms
1 pA/pF
100 ms
b
+ 90 mV
τ (ms)
Control
Washout
c
-80 mV
τ (ms)
Control
Washout

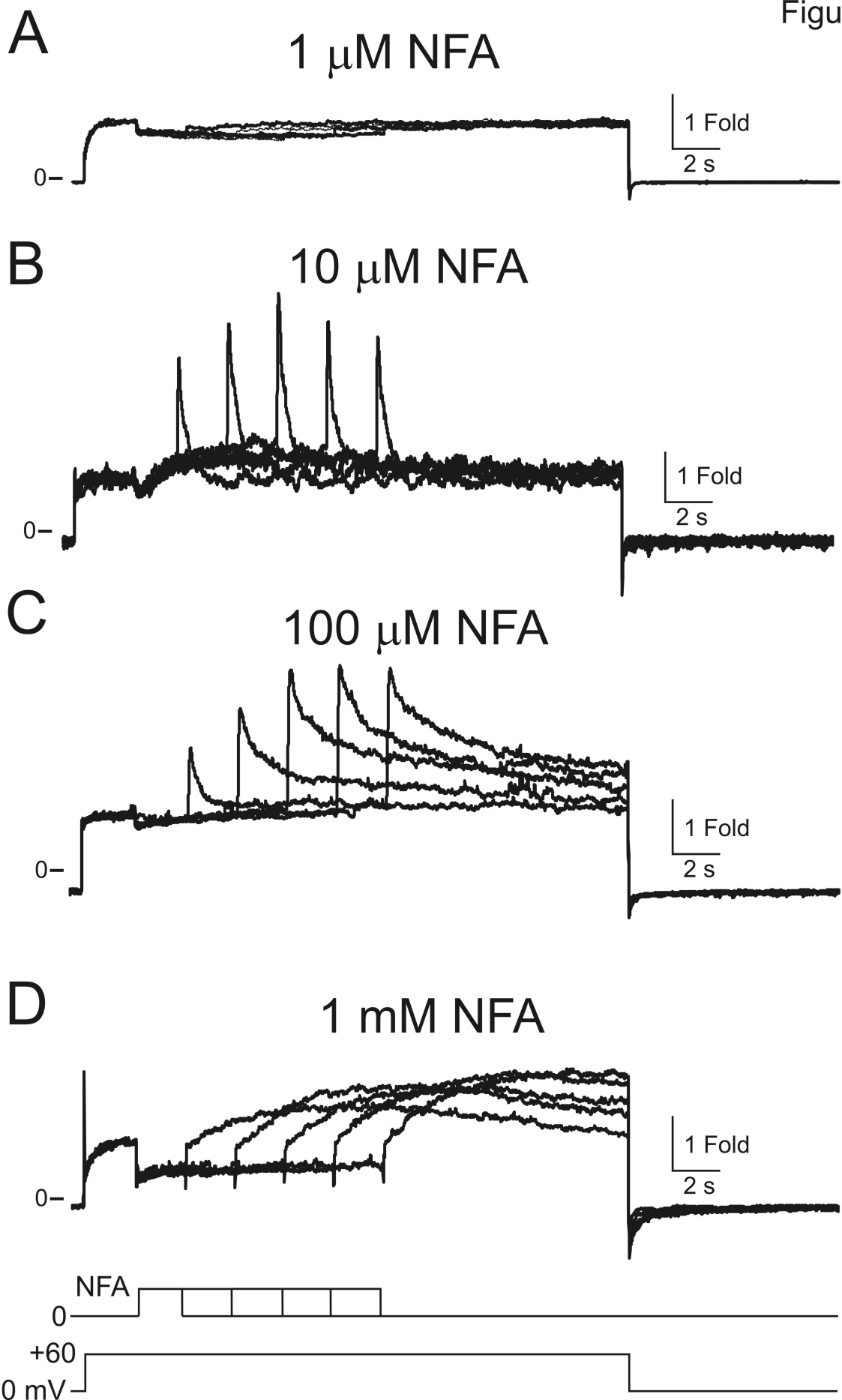
A
1 μM NFA
1 Fold
2 s
0
B
10 μM NFA
1 Fold
2 s
0
C
100 μM NFA
1 Fold
2 s
0
D
1 mM NFA
1 Fold
2 s
0
NFA
0
+60
-50 mV

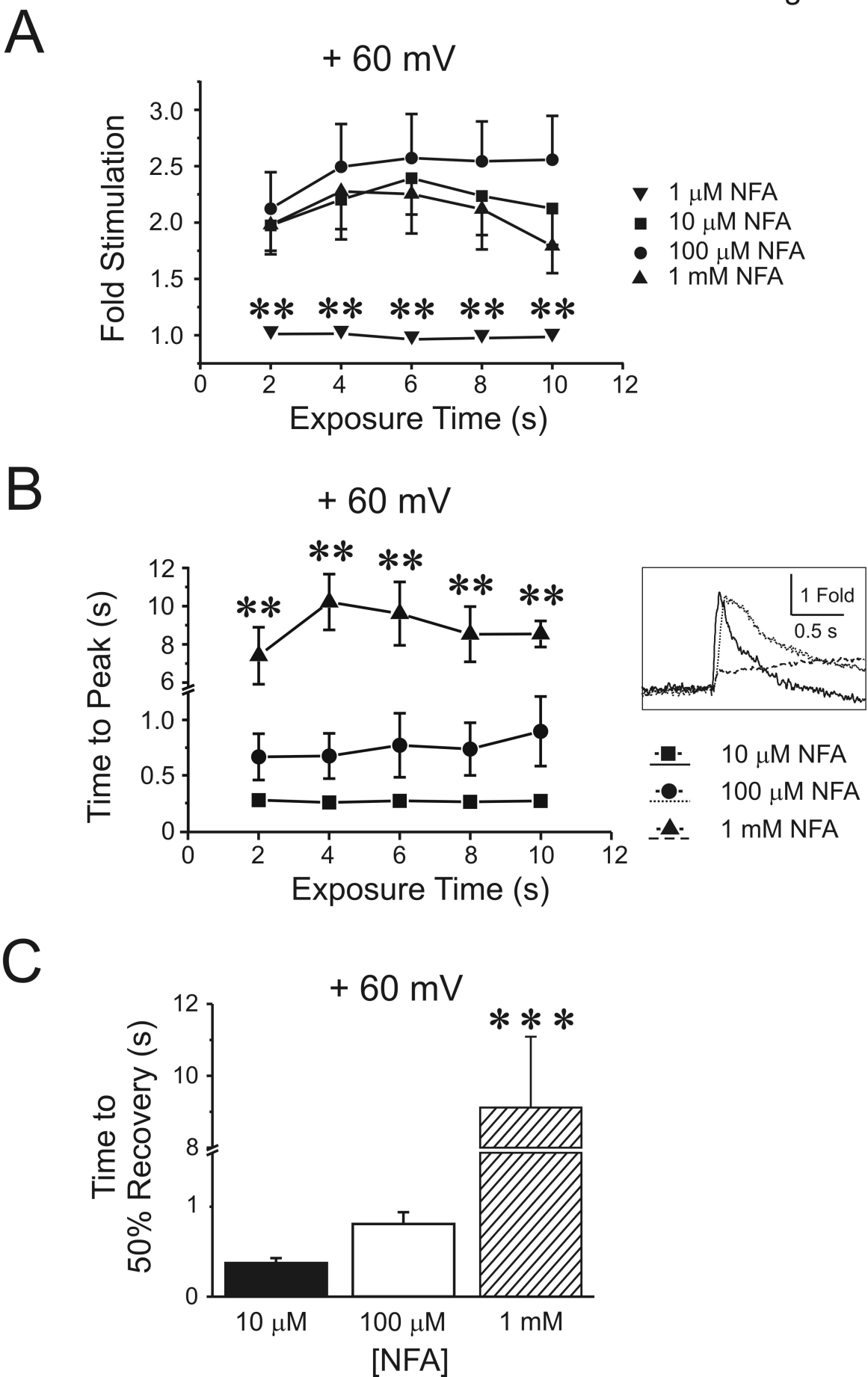
A
+ 60 mV
Fold Stimulation
3.0
2.5
2.0
1.5
1.0
0
2
4
6
8
10
12
Exposure Time (s)
1 μM NFA
10 μM NFA
100 μM NFA
1 mM NFA
B
+ 60 mV
Time to Peak (s)
12
10
8
6
1.0
0.5
0
Exposure Time (s)
1 Fold
0.5 s
10 μM NFA
100 μM NFA
1 mM NFA
C
+ 60 mV
Time to 50% Recovery (s)
12
10
8
1
0
10 μM
100 μM
1 mM
[NFA]

Figure 4

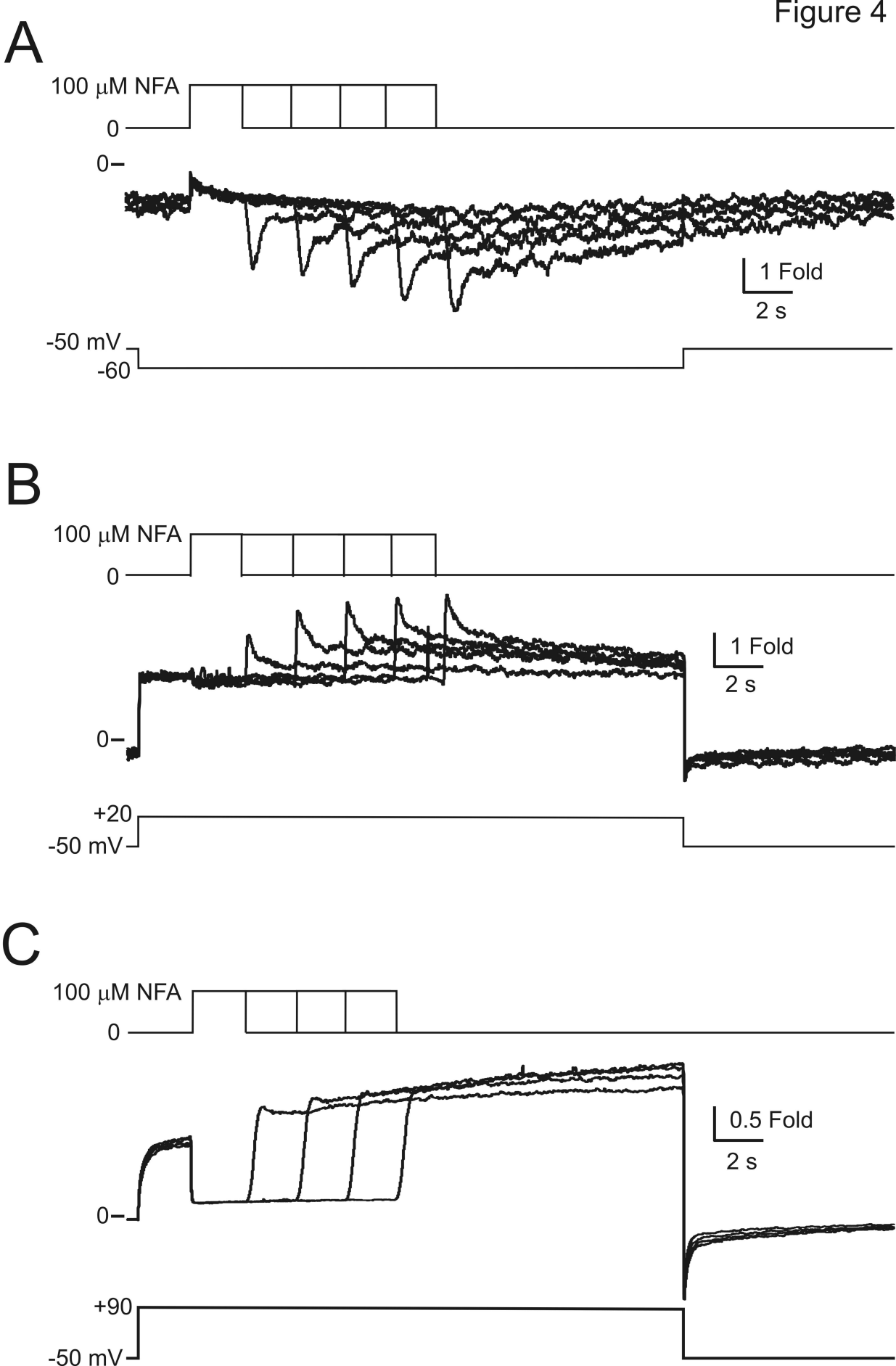
A
100 μM NFA
0
0
1 Fold
2 s
-50 mV
-60
B
100 μM NFA
0
1 Fold
2 s
0
+20
-50 mV
C
100 μM NFA
0
0.5 Fold
2 s
0
+90
-50 mV

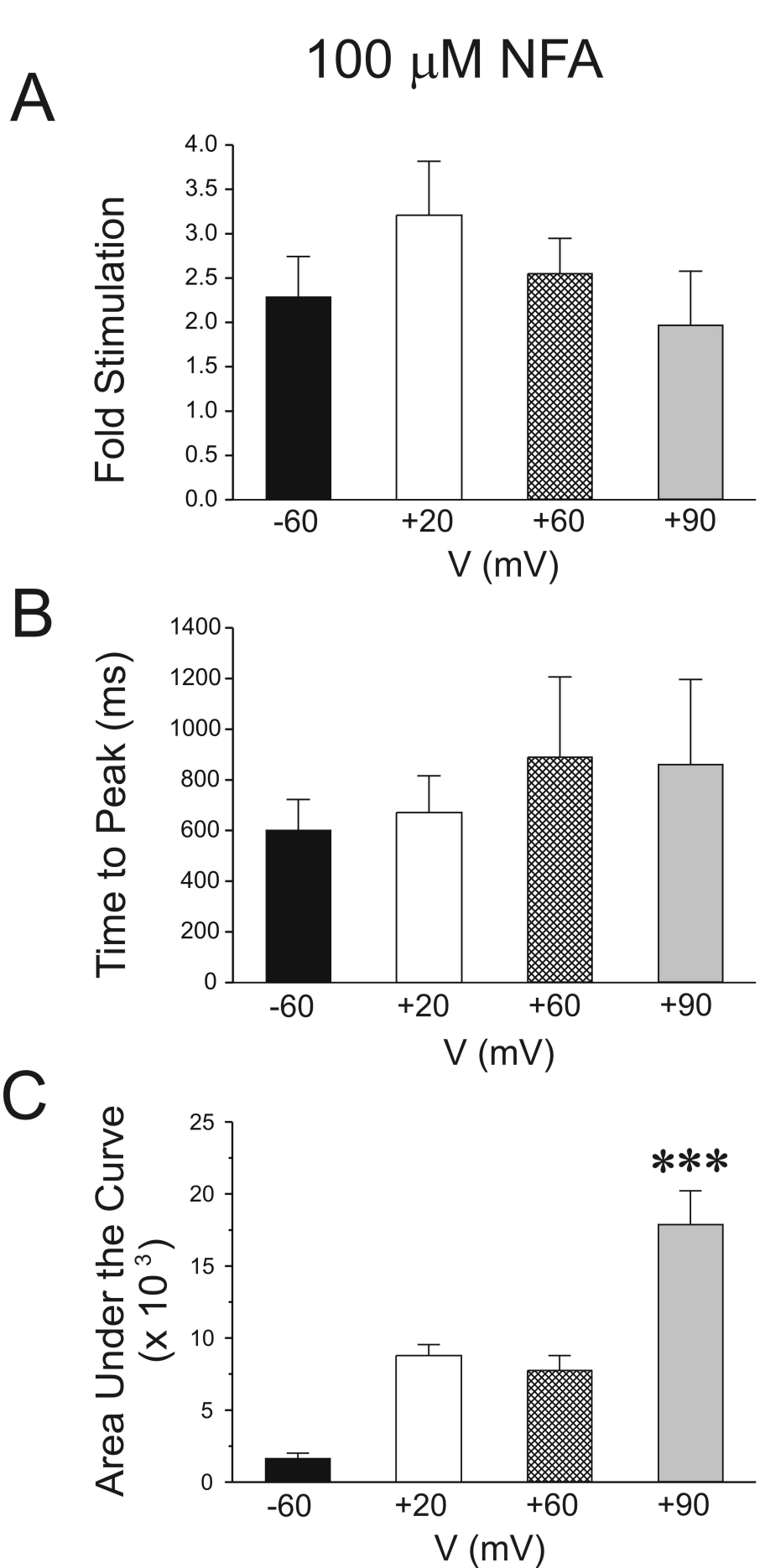
100 μM NFA
A
Fold Stimulation
4.0
3.5
3.0
2.5
2.0
1.5
1.0
0.5
0.0
-60
+20
+60
+90
V (mV)
B
Time to Peak (ms)
1400
1200
1000
800
600
400
200
0
-60
+20
+60
+90
V (mV)
C
Area Under the Curve
(x 10 3)
25
20
15
10
5
0
***
-60
+20
+60
+90
V (mV)

A

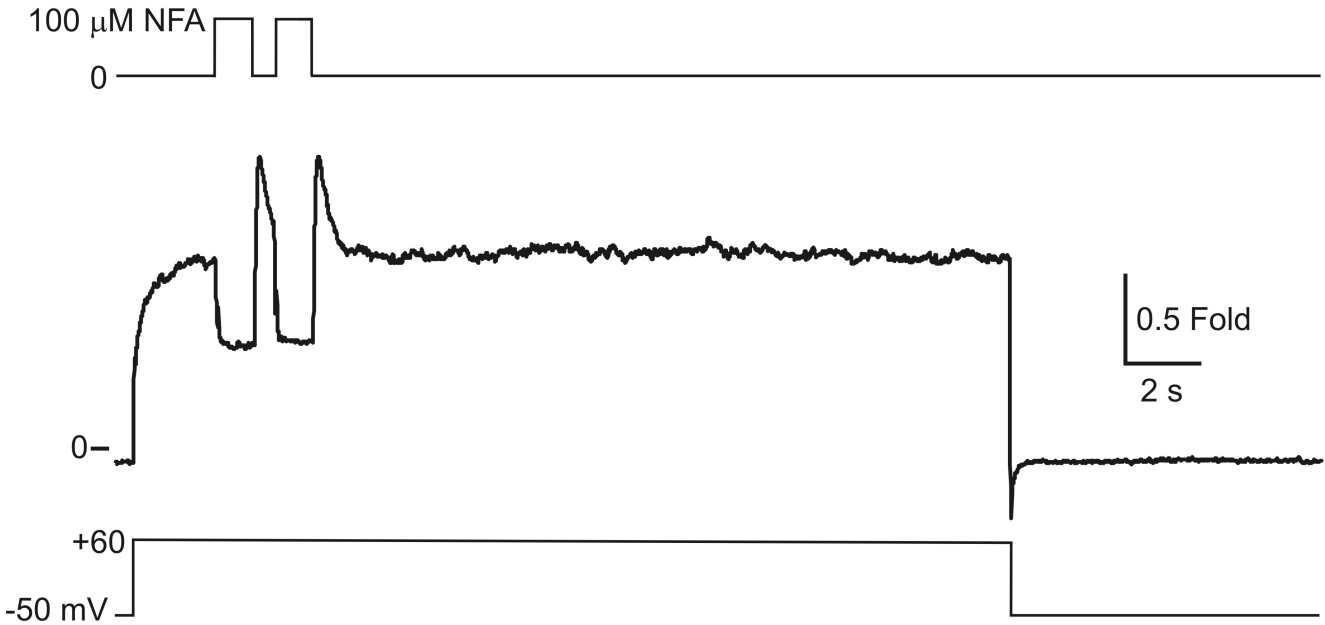
100 μM NFA
0
0.5 Fold
2 s
0
+60
-50 mV

B

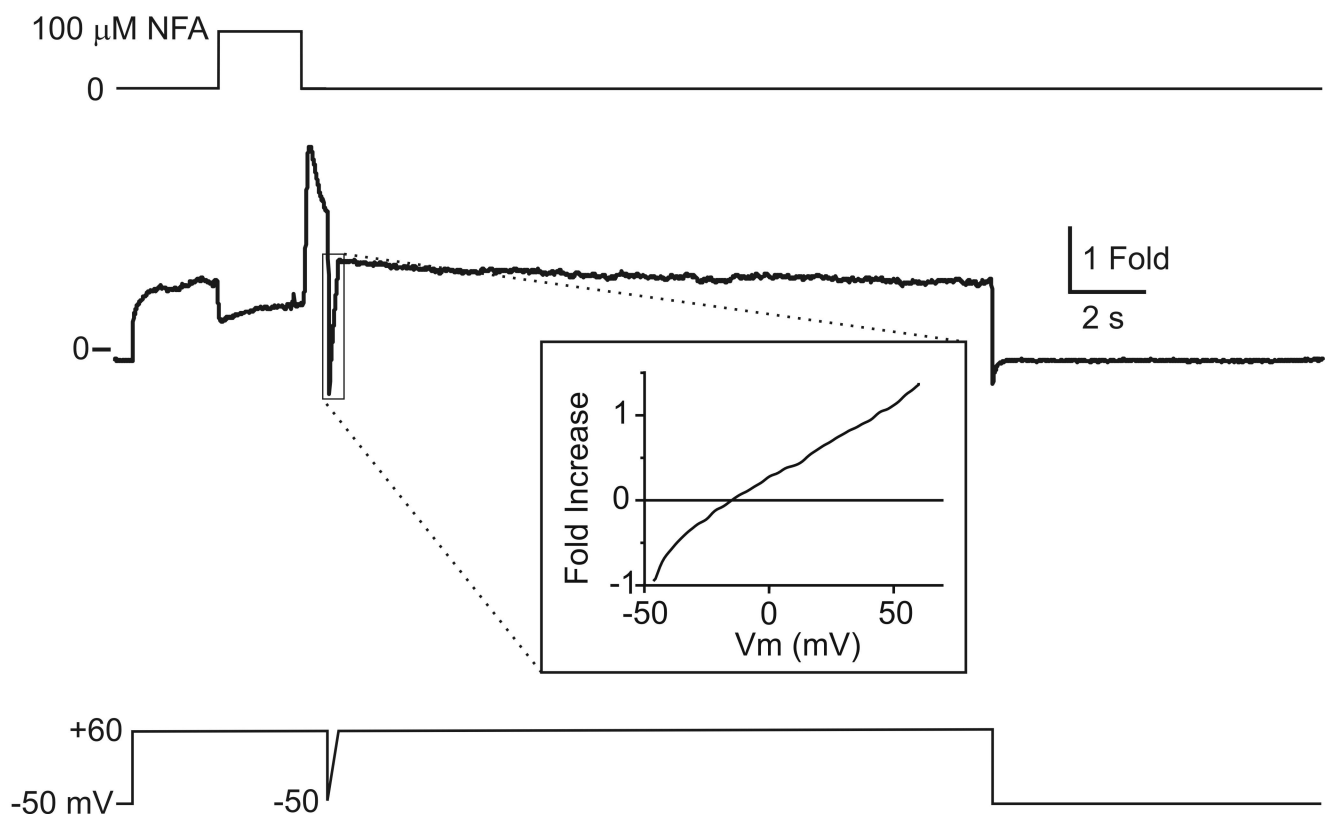
100 μM NFA
0
1 Fold
2 s
0
Fold Increase
1
0
-1
-50
0
50
Vm (mV)
+60
-50 mV
-50

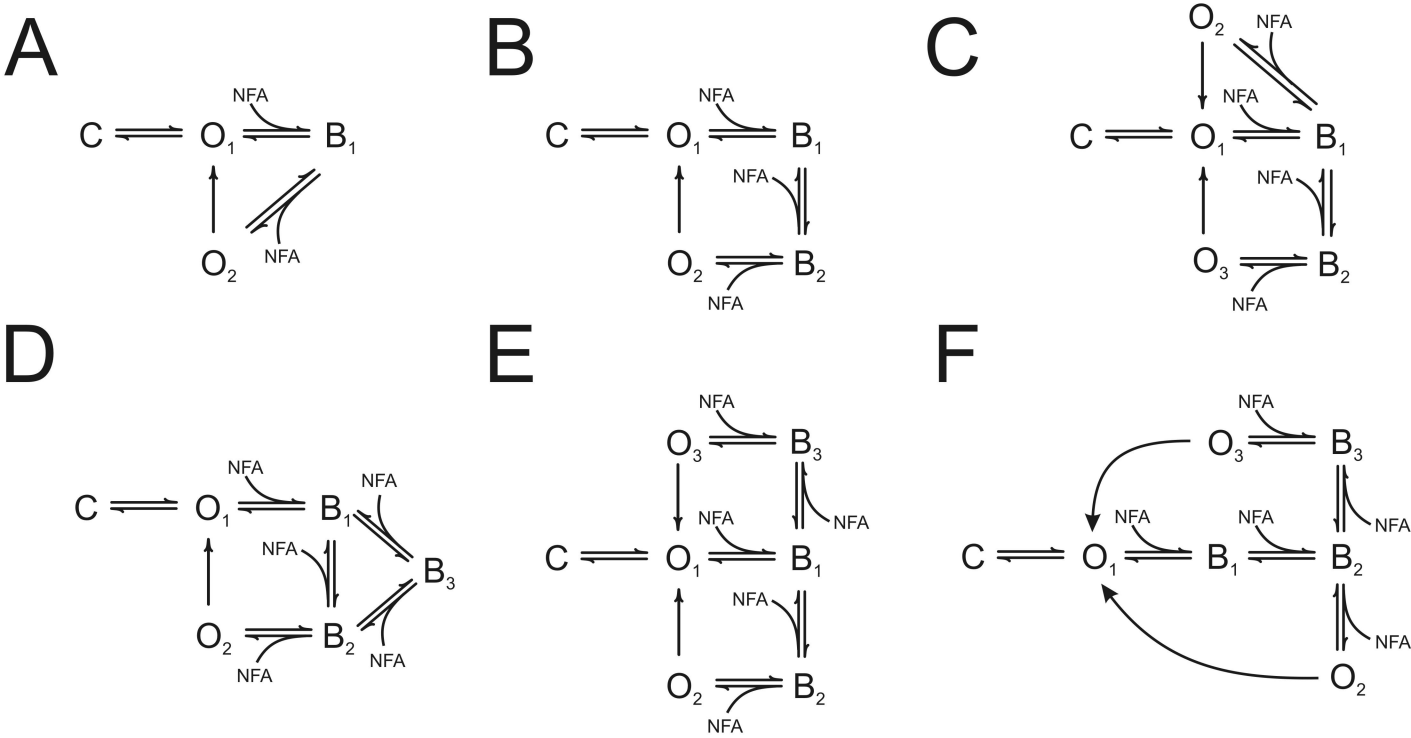
A
B
C
D
E
F
NFA
C
O1
O2
O3
B1
B2
B3

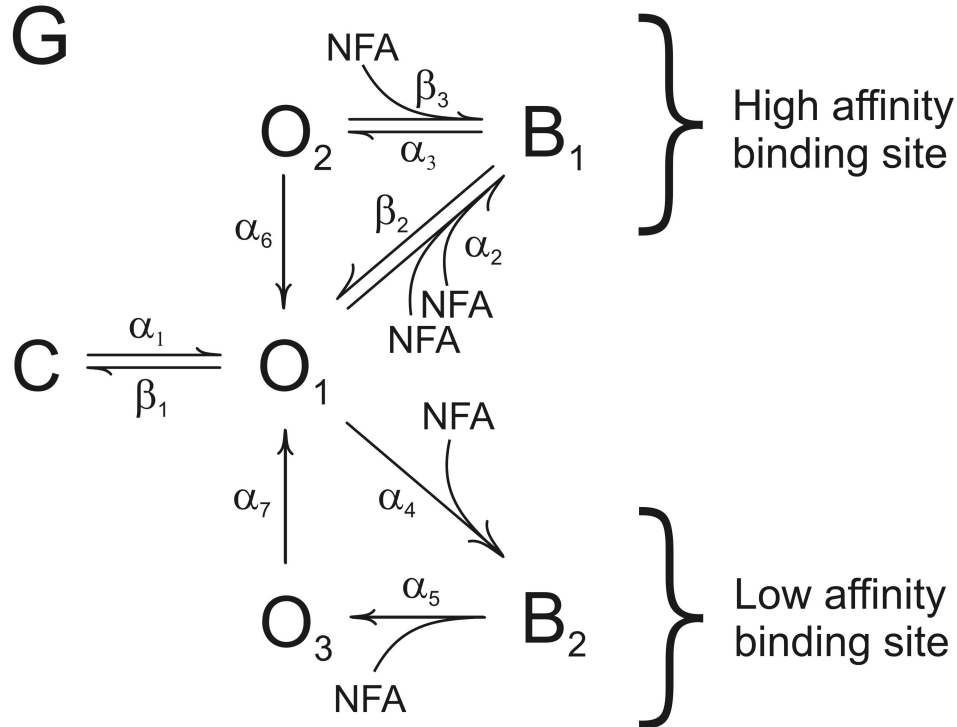
G
NFA
β3
α3
O2
B1
α6
β2
α2
NFA
NFA
C
α1
β1
O1
NFA
α7
α4
α5
O3
B2
NFA
High affinity binding site
Low affinity binding site

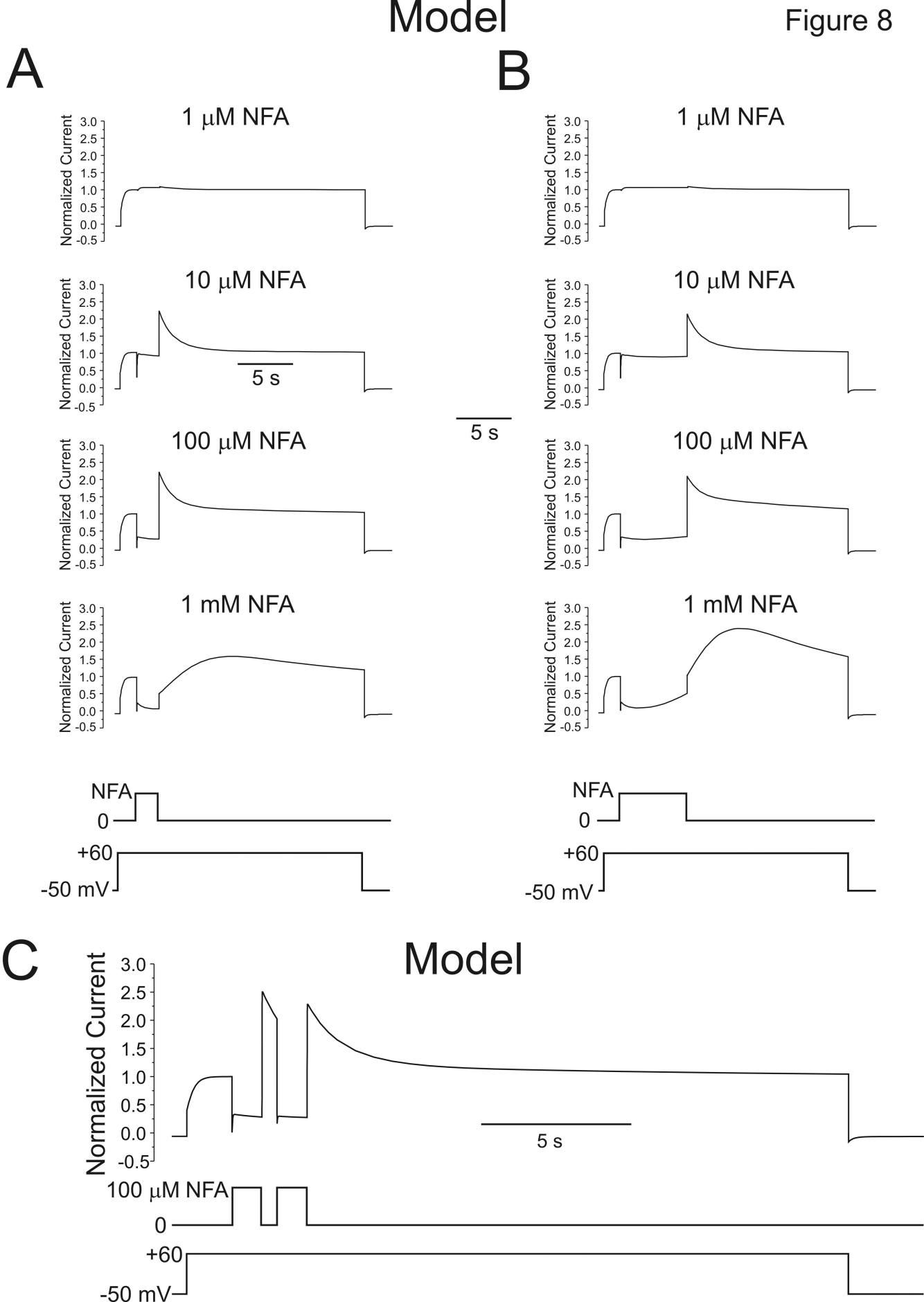
Model
A
B
1 μM NFA
10 μM NFA
100 μM NFA
1 mM NFA
Normalized Current
3.0
2.5
2.0
1.5
1.0
0.5
0.0
-0.5
5 s
NFA
0
+60
-50 mV
C
Model
Normalized Current
100 μM NFA
0
+60
-50 mV
5 s

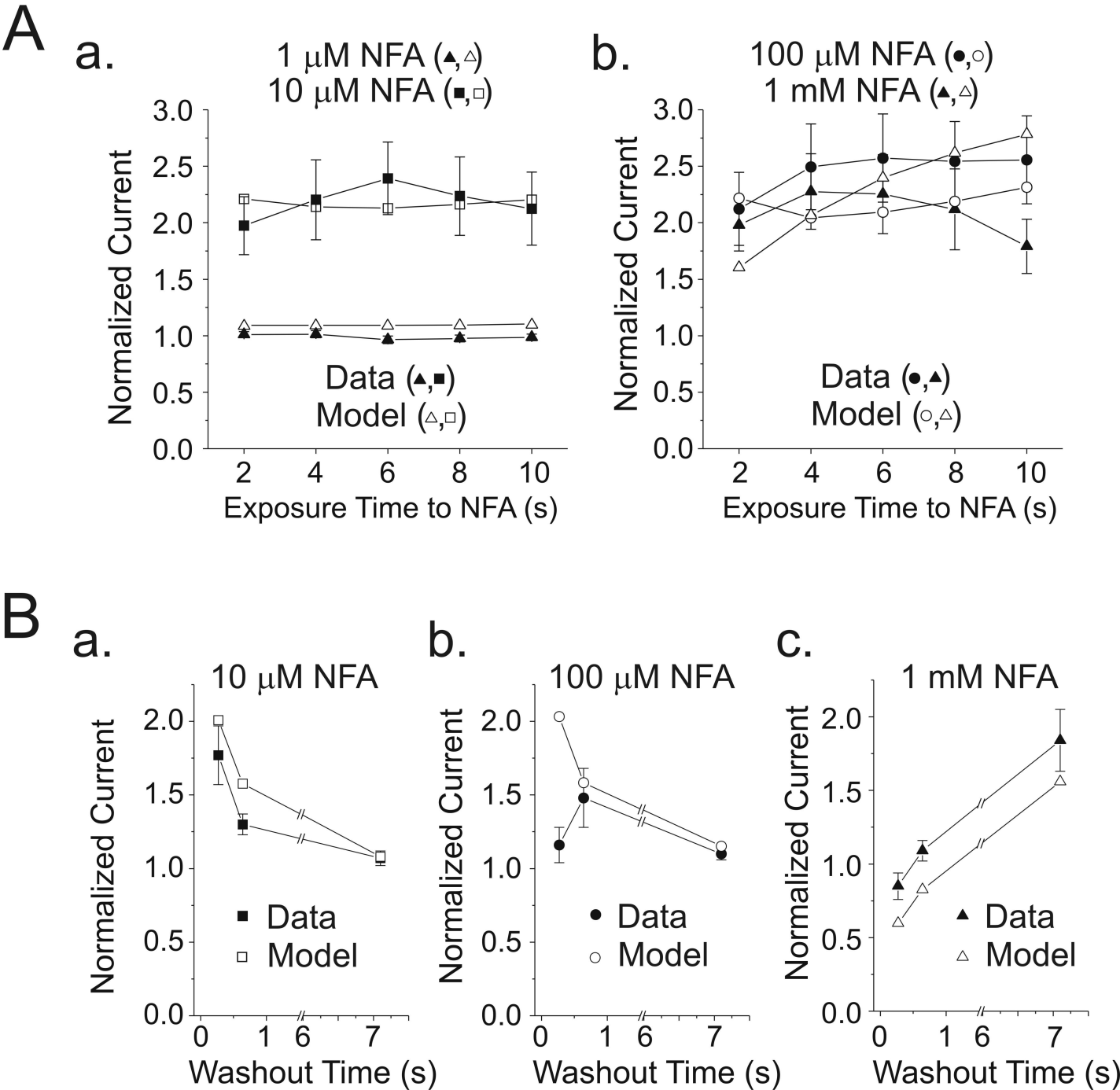
A
a.
1 μM NFA (▲,△)
10 μM NFA (■,□)
Normalized Current
Data (▲,■)
Model (△,□)
Exposure Time to NFA (s)
b.
100 μM NFA (●,○)
1 mM NFA (▲,△)
Normalized Current
Data (●,▲)
Model (○,△)
Exposure Time to NFA (s)
B
a.
10 μM NFA
Normalized Current
Data
Model
Washout Time (s)
b.
100 μM NFA
Normalized Current
Data
Model
Washout Time (s)
c.
1 mM NFA
Normalized Current
Data
Model
Washout Time (s)